Conf-911123--3

Irradiation behavior of metallic fast reactor fuels*

R. G. Pahl, D. L. Porter, D. C. Crawford, and L. C. Walters

Fuels and Engineering Division,

Argonne National Laboratory,

Idaho Falls, ID 83402-2528

MASTER

DISCLAIMER

Irradiation behavior of metallic fast reactor fuels[*]

R. G. Pahl, D. L. Porter, D. C. Crawford, and L. C. Walters

Fuels and Engineering Division, Argonne National Laboratory, Idaho
Falls, ID 83402-2528

Metallic fuels were the first fuels chosen for liquid metal
cooled fast reactors (LMR's). In the late 1960's world-wide interest
turned toward ceramic LMR fuels before the full potential of metallic
fuel was realized. However, during the 1970's the performance
limitations of metallic fuel were resolved in order to achieve a high
plant factor at the Argonne National Laboratory's Experimental Breeder
Reactor II. The 1980's spawned renewed interest in metallic fuel when
the Integral Fast Reactor (IFR) concept emerged at Argonne National
Laboratory. A fuel performance demonstration program was put into place
to obtain the data needed for the eventual licensing of metallic fuel.
This paper will summarize the results of the irradiation program carried
out since 1985.

1. Introduction

A critical review [1] of the performance of metallic fuels and blankets in liquid metal fast breeder reactors was published in May of 1984. In it, the authors identified what they believed to be the most attractive system for further metallic fuel development: U-Pu-Zr fuel clad with an advanced stainless steel alloy. At that time only 18 U-Pu-Zr fuel elements had been irradiated in excess of 1 atomic % heavy metal burnup, with the highest exposure equal to only 5.6 at. % burnup. While the observed performance was very encouraging, the data base was lacking in comparison to the leading concept of the time, ceramic fuel. In order to achieve a competitive position with other fuel types, plutonium-bearing metallic fuel would have to be irradiated to high burnup in statistically significant numbers and demonstrate their reliability during steady state, transient and breach conditions.

In February of 1985, Argonne National Laboratory embarked on an aggressive irradiation program to accomplish this goal when the first of the post-1960's U-Pu-Zr fuel was loaded into the core of the Experimental Breeder Reactor II (EBR-II). These experiments [2] were to become the first in a series of tests designed to demonstrate reliable fuel performance in support of the Integral Fast Reactor Program (IFR) [3] at ANL.

During the subsequent seven years, an extensive in-reactor test program has evolved. The irradiation of over 600 plutonium-bearing

metallic fuel elements of various designs has been completed or is now in progress at EBR-II. High performance cladding alloys have been tested, including 20% cold-worked D9 (a titanium-modified austenitic stainless steel) and HT9, (a low-swelling ferritic/martensitic alloy). Contributing to the database and providing a high plant factor for EBR-II, over 13,000 U-10Zr test and standard driver fuel elements have been irradiated. Qualification testing of the Mark-III (U-10Zr fuel with 20% cold-worked D9 cladding), Mark-IIIA (U-10Zr fuel with 20% cold-worked Type 316 cladding), and Mark-IV (U-10Zr fuel with HT9 cladding) EBR-II driver fuel options is nearing completion and will be described in a future publication. In addition, successful tests of prototypical U-Pu-Zr fuel elements in the Fast Flux Test Facility (FFTF) have been carried out, with excellent fuel performance demonstrated for a ~one meter core height. The lead D9-clad U-0,8,19Pu-10Zr fuel elements reached goal burnup of 10 at. % without breach in the IFR-1 test in FFTF. The lead HT9-clad binary fuel (U-10Zr) is currently approaching 15 at. % burnup in FFTF in the MFF-1 test. A total of seven HT9-clad binary fuel tests have been carried out to qualify a potential metallic driver fuel core for FFTF. Results from the FFTF tests are being compiled for publication at a later date. Endurance tests of HT9-clad metallic fuel in EBR-II are nearing the 20 at. % burnup level without a single breach, and an ongoing run-beyond-cladding-breach program has demonstrated the benign breach behavior of metallic fuel.

This paper will summarize what has been learned about metallic fuel performance as a result of this steady-state irradiation test program at ANL. The next section will describe the evolution of

metallic fuel design that has enabled high burnup performance from IFR fuel. The subsequent sections will then describe specific tests which were designed to broaden the database to a wider range of operating, design and fabrication variables and a recent analysis of IFR fuel breach behavior. While beyond the scope of this paper, a parallel effort at ANL addresses the related issues of transient fuel behavior [4] and high temperature fuel/cladding compatibility [5].

2. Metallic Fuel Design

Lessons learned from studying EBR-II driver fuel and cladding performance have contributed greatly to the high burnup capability of today's metallic fuel elements. The original EBR-II driver fuels were the Mark-I/IA types. They consisted of a U-5Fs alloy fuel slug, bonded with sodium to effect heat transfer, and clad in a solution annealed Type 304L jacket. Fissium (Fs) is a 2.4Mo-1.9Ru-0.3Rh-0.2Pd-0.2Zr-0.01Nb alloy (wt %). This fuel alloy was chosen for its low swelling properties and represented the equilibrium alloy for the pyrometallurgical process then in development at EBR-II. A plenum-to-fuel volume ratio of only 0.19, 85% smeared fuel density (fraction of the cladding inside diameter taken up by fuel), and a cladding wall thickness of only 0.23 mm contributed to a maximum usable burnup of only ~3%. Fuel swelling could not be restrained and fuel column breaches occurred. Also, the solution annealed Type 304L alloy has a very short incubation fluence for swelling and would have eventually been limited to low burnup by bundle-duct interaction, even if the creep strain had been minimized by proper design.

4

A very simple but very significant design breakthrough for EBR-II driver fuel took place in 1973 when the smeared density was lowered from 85% to 75%. If fuel swelling from fission-gas bubble growth is allowed to exceed ~30%, most of the gas is released from the fuel to the plenum rather than being trapped in high pressure bubbles. This gas release results in a relatively spongy fuel which can be restrained by even moderately strong cladding. Because only ~17% swelling was allowed in radial directions prior to fuel/cladding contact in the Mark I/IA design, gas release was limited to ~2% or less. In a 75% smeared density fuel element, fuel cladding contact first occurs at ~33% radial swelling. Thus, gas release at point-of-contact is substantial and fuel/cladding mechanical interaction (FCMI) is negligible. This type of behavior has been experimentally verified in the late 1960's tests of many metallic fuel alloys over a wide range of conditions and is observed in today's tests of IFR fuel as well. The onset of rapid gas release coincides with the interconnection of porosity and fuel/cladding contact as is shown in figure 1 for typical IFR fuel. Details of the swelling characteristics and gas release behavior in typical IFR fuel of today's design have previously been described [2].

Realizing the importance of the design considerations discussed above, ANL designers lengthened the driver fuel element to 612 mm raising the plenum-to-fuel volume ratio to 0.82 (still somewhat small by today's standards), reduced the smeared density to 75%, and used thicker (0.30 mm) cladding. Both Type 304L and Type 316 cladding were tested, with solution annealed Type 316 eventually becoming the reference choice

for the Mark-II driver fuel. The resulting increases in burnup capability were remarkable. The breach threshold for Mark-II fuel was ~10 at. % burnup and allowed EBR-II to operate with an enviable plant factor during the 1970's and 1980's.

However, the weak link in the Mark-II design was never corrected, even though it was well-characterized. In order to limit axial fuel motion ("liftoff"), a dimple was mechanically pressed into the cladding ~12.7 mm above the fuel column. Failure, though completely benign, typically occurred at this feature which acted as a stress concentrator. Little incentive existed for increasing the Mark-II burnup capability by modifying the restrainer, due to the fact that the fuel assembly exposure was limited by dilation of the outer hexagonal-duct which must fit into the in-reactor storage basket after irradiation. Experience has shown that axial fuel motion is self-limiting and restrainers are now considered unnecessary.

Today, all EBR-II driver fuel and IFR prototype fuel elements lack a restrainer and possess a properly sized plenum and cladding wall thickness to limit stress to manageable levels over the element lifetime. Most of the performance data accumulated to date were obtained from elements clad with the D9 and HT9 alloys. The result of these design changes and materials choices are fuel elements which exhibit low levels of cladding strain. Diametral cladding strain which results from in-reactor creep deformation and irradiation-induced swelling.is a useful figure of merit one can use to judge high burnup capability of fuel elements. High creep strains can indicate high damage fractions in

the material and increasing probability of stress rupture failure. High swelling strains, while not damaging per se, correlate with reliability issues related to diminishing bundle/duct clearances.

D9-clad and HT9-clad IFR elements exhibited lower diametral cladding strain than did 304L-clad or 316-clad Mark-II elements (Figure 2). Beginning of life peak inside cladding temperatures for the Mark-II data ranged from ~550°C for the Type 304L to ~590°C for the Type 316. The IFR element temperatures were comparable, ranging from ~540°C to ~580°C for the D9 to ~590°C for the HT9. The upper two curves show the large strain experienced in the Mark II design U-5Fs fuel for Type 304L and Type 316 cladding. Approximately 80% of this strain results from swelling. The lower curves show data taken from the lead D9-clad tests (X419, X420, X421) [2] and the lead HT9-clad test (X425) [5]. Recent immersion density data obtained from an X421 element with U-19Pu-10Zr fuel at ~17.8 at. % burnup indicates that ~40% of the total peak strain in the D9 cladding is due to swelling (about twice that predicted in reference [2] for sibling fuel), and extensive in-reactor tests of HT9 to high fluence indicate that swelling for the HT9 cladding in the X425 test at the burnup levels shown in Figure 2 should be negligible. Therefore, the difference in deformation behavior seen in Figure 2 is attributable mostly to better swelling behavior of the D9 and HT9 materials. The superiority of the D9 and HT9 for high fluence applications is clear from this plot and illustrates the progress made in reducing cladding strains by proper design and material selection.

While the Mark-II breach threshold was ~10 at. % burnup, the first breach in the D9-clad elements occurred in the closure weld of a poorly designed end plug at ~13.5 at. % burnup [2]. The first fuel column breach occurred at ~16.4 at. % with plenum breaches observed between ~14.5 at. % and ~17 at. % burnup. At test termination, the peak D9-clad element attained ~18.4 at. % peak burnup without breach. The HT9-clad test, X425, is now approaching ~20 at. % burnup. None of the elements in this experiment have breached. Because the lead D9 and HT9 tests were performed under a limited range of operating conditions, a series of tests followed to explore the effects of various design, operating and fabrication variables on fuel performance. The important results from these tests are summarized in the following sections.

3. Design, operating and fabrication variables testing

This section summarizes the results of 5 recent experiments carried out in EBR-II. Test objectives in the X447 test centered on determining the burnup capability of HT9 cladding at extremely high cladding temperature, 660°C (Table 1) [6]. Ternary driver fuel design variables were studied in the X441 test by systematically varying plenum-to-fuel volume ratio, smeared density, and fuel composition (Table 1) [6]. A pair of companion tests, X431 and X432 are being used to study the effects of design parameters on metallic blanket fuel behavior. Interim examination results are being reported here for the first time. The feasibility of using consumable fuel casting molds made from thin zirconium tubes is currently being investigated with the X492 test. Their low burnup performance is also being reported here for the

first time. Finally, a brief discussion of recent analyses of run-beyond-cladding breach is presented.

3.a High temperature performance of HT9-clad binary fuel

One interim examination was completed on X447 elements at the 4.7 at. % burnup level. Cladding strain was negligible over most of the fuel column except at the top-of-core, where the peak diametral strain was ~0.80%. Optical metallography and electron microprobe wavelength dispersive x-ray analysis showed significant fuel/cladding chemical interaction. Lanthanide series elements were found to a depth of ~0.07 mm in the cladding in the hotter portions of the cladding. Destructive post-irradiation examinations of X447 fuel at ~10 at. % burnup are now in progress and will be reported in detail in a future publication. Fission gas pressure data showed ~75% release at this burnup level, consistent with the data from Figure 2. The cladding strain profiles were similar in shape to the 4.7 at. % burnup data, except that the total strain had doubled to ~1.6% on the average in unbreached elements.

Two elements have breached in the X447 test at ~9.5 at. % burnup. The average strains measured at the top-of-core where breach occurred were ~1.6% and ~4.1%. These strains fall into the normal range of (thermal) failure strains for the HT9 alloy. Even though the observed breach behavior in X447 was benign, the lifetimes of HT9-clad elements at 660°C are short due to the high levels of thermal creep strain. The amount of cladding wastage by FCCI and its contribution to the breaches has yet to be determined.

9

3.b Design variables testing of ternary fuel

Subassembly X441 was designed to test the variables shown in Table 1. This test was expressly designed to benchmark the fuel performance code LIFEMETAL [5] and was run to a peak burnup of ~12.7 at. % with no breached elements. As can be seen from Table 1, the end-of-life diametral strain in all but the high smeared density set of elements was small (0.17% to 0. 1%), indicating negligible fuel/cladding mechanical interaction and an adequate plenum volume and cladding strength to accommodate the fission gas pressure. Also apparent is the beneficial effect of raising the plenum-to-fuel volume ratio and keeping the smeared density at 75% or lower. The effect of zirconium (which is believed to enhance cladding chemical compatibility and raise the solidus temperature) in the fuel does not appear in the cladding strain data but may show up in high temperature fuel/cladding compatibility tests which are now in progress. Optical metallography of the U-19Pu-10Zr fuel at 11% peak burnup (75% smeared density) revealed the usual lanthanide-rich diffusion band (up to 0.058 mm deep) in the HT9 cladding. What role this interaction layer plays in high temperature off-normal events is currently under unvestigation [5]. Besides providing data for the LIFEMETAL code, this test has demonstrated excellent performance characteristics for future IFR driver fuel candidates as the design variables and operating conditions tested envelope much of that expected in a reference design.

3.c Metallic blanket element design testing

Although the reference fuel design for IFR driver fuel has been determined to be a U-Fu-Zr fuel slug clad in an advanced cladding alloy, the design choices for metallic blanket fuel are still open because so little pertinent data on metallic blanket fuel exists. Although HT9 steel appears to satisfy blanket cladding requirements, the optimal choice of fuel composition and smeared density is not clear. Increasing the uranium content by lowering the Zr would be advantageous from the standpoint of Pu breeding but applicable data on low Zr fuel is sparse. The objectives for the X431 and X432 blanket assembly irradiation tests were to: 1) investigate the effects of smeared density and fuel composition on blanket element behavior to prototypic goal burnup. 2) generate performance data which will be used to benchmark the LIFEMETAL fuel performance code, especially regarding FCMI in high smeared density applications. and 3) provide irradiated test elements for ex-reactor high temperature tests.

The X431 and X432 tests utilize two smeared densities (85% vs 90%) and three fuel alloy contents (U-2,6,and 10% Zr). Each 19-element subassembly contained 2 to 5 elements from each of the 6 groups described in Table 3. All 6 types were wire-wrapped HT9-clad elements ~0.98 mm long x ~9.4 mm in diameter. The fuel slugs in all 6 types were nominally 343 mm x 7.95 mm. Smear density was thus controlled by varying the cladding wall thickness. U235 enrichment was adjusted to give each fuel type the same power, given by: 8.5% (U-2Zr), 10.7% (U-6Zr), and 13.2% (U-10Zr). Both subassemblies were irradiated in row 4 of EBR-II at

a peak midplane linear power of ~ 39.4 kW/m. The peak inside cladding temperature was ~600°C for both subassemblies. The two subassemblies were removed at ~30% of their goal burnup of 5% for interim examination. Axial fuel growth measurements made from neutron radiographs, and the averaged results are summarized in Table 3. For a given level of burnup and Zr addition, high smeared densities promote low axial growth levels. Considering that the fuel/clad gap was closed except at the very top of the fuel column, free swelling in the axial direction seems to be effectively shut off once the gap is closed.

The cladding diameter profiles were measured by spiral contact profilometry after irradiation. This technique measures the diameter at 90° to the spacer wire. The average response is summarized in Table 3. Essentially no measurable dilation occurred in the plenum region where deformation would be caused by gas loading alone. This indicates that the observed cladding deformation is mainly due to FMCI. For all fuel alloys, the 90% smeared density elements showed more strain in spite of their thicker walls. This is to be expected if FMCI dominates fission gas loading.

Zirconium content did not appear to significantly affect the cladding deformation at these burnups. However, four of the five U-2Zr 85% smeared density elements showed pronounced ovality and large cladding strains at the bottom ~2.5 inches of the fuel column. A possible source of stress resulted from localized grain coarsening in the fuel column during irradiation. Metallographic examination revealed that the originally fine-grained structure seen in the as- cast fuel had

evolved into a coarse columnar-grained structure over as much as 50% of the fuel cross section. No FCCI was observed and microhardness data on the HT9 was uniform at a given elevation and normal in magnitude, indicating that the thermal history was not suspect. The authors believe that this stess resulted from preferred growth along the [010] direction of the orthorhombic uranium grains. This preferred growth could be due to either irradiation growth or thermally activated grain growth.

In summary, good performance characteristics have been observed in the high smeared density U-Zr blanket fuel tested to ~1/3 of goal burnup. With one exception, their behavior has been consistent regarding expected cladding and fuel strain. Fuel/cladding compatibility was good. No breaches have been incurred at this burnup level. Anomalous cladding strain behavior has been observed in U-2Zr, 85% smeared density fuel. The X431 and X432 tests are now at 2.7 at. % and 3.2 at. %, respectively and will continue irradiation to goal burnup of 5 at. % or first natural breach. The results of these tests will be reported in greater detail in the future.

3.d Zirconium-sheathed fuel tests

The current fabrication process involves casting IFR fuel into quartz molds. Because the quartz molds are destroyed during the fuel demolding process, the quartz residue must be treated as a contaminated waste stream. Alternatively, if the fuel could be cast into molds that can remain intact as an integral part of the fuel slugs (i.e., if the fuel can be left inside the molds for irradiation), then the quartz mold

13

contribution to the waste stream will be eliminated [7]. This possibility is being addressed in an on-going effort to evaluate the irradiation performance of fuel cast into zirconium tubes or sheaths rather than quartz molds. Zirconium was chosen as the sheath material because it is the component of the U-Pu-Zr fuel alloy that raises the alloy solidus temperature and provides resistance against fuel cladding chemical interaction. Thus, the Zr sheath was expected to provide a compatible barrier to FCCI as well as a mold alternative.

Binary (U-3Zr) and ternary (U-20.5Pu-3Zr) fuel alloys were cast into Zr tubes in fuel fabrication facilities at ANL-W. The sheathed slugs were designed to have dimensions similar to standard production Mark-IIIA slugs. The Zr content of the melt was reduced to account for the Zr in the sheath, giving the binary sheathed slugs an overall composition of ~U-10Zr and the ternary sheathed slugs an overall composition of ~U-19Pu-10Zr. The Zr-sheathed fuel slugs and normal production slugs of U-10Zr and U-19Pu-10Zr were clad in standard MK-IIIA hardware (20% cold-worked Type 316), loaded into a 61-element subassembly, (X492), and irradiated in EBR-II to a peak burnup of 1.95 at. % .

The Zr-sheathed slugs exhibited significantly less axial growth (averaging 1.3% for the ternary alloy and 1.8% for the binary alloy) than did the quartz-mold slugs (4.9% and 8.1%, respectively). Transverse metallography sections at x/L_0 ~ 0.23 and ~0.78 of a U-20.5Pu-3Zr Zr-sheathed element reveal wedge-shaped longitudinal cracks, presumably running down the length of each of the two slugs. Electron

14

microprobe wavelength dispersive x-ray analysis determined the Zr concentration of the dense zone in the center of the element to be roughly 0.5 wt %, depleted from the 3 wt % Zr content for the fuel alloy, and that of the porous fuel lying between the Zr sheath and the dense center zone to be 5 to 6 wt %. Although the two transverse sections show no fuel-clad contact through the opened crack, the fuel approaching the cladding through the crack was determined to have as little as 1.1 wt % Zr.

Although the results show that Zr sheaths, in the form tested, cannot be a reliable barrier to FCCI because of cracking, two other advantages hold promise for the concept. First, fuel slugs can be cast into Zr tubes, eliminating the need for quartz molds. Second, the Zr sheaths appear to reduce axial growth to strains below 2%. This is beneficial for reactor reactivity considerations. Furthermore, if the low Zr fuel in the sheathed elements does in fact interact with cladding in a manner that causes premature failure, then variations of the concept can still be pursued. For example, the Zr content of the fuel alloy can be increased to, say, 6 wt %. Such a fuel alloy has performed well in the X441 test, so there may be no need to rely on a Zr sheath to ensure fuel/cladding compatibility. If fuel can be cast into thinner Zr tubes, then the "smeared" composition of 10 wt. % Zr can be retained by casting 6 wt % Zr fuel into Zr tubes with proportionally thinner walls.

3.e Run-beyond cladding breach (RBCB) performance

The characterization and monitoring of IFR fuel breaches is now a significant part of the IFR fuel testing program at EBR-II. Benign behavior has been reported in all of the intentional and natural breaches studied to date [8] [9]. Reactor operations at EBR-II have continued for months with breached metallic fuel in the core because of low fission gas activity and no breach extension or fuel loss to the coolant. Reference [8] described the most recent phase of the RBCB program, an analytical effort aimed at differentiating the fission gas release with regard to breach type, ie. stored-gas release, diffusional release, or direct recoil release. By analyzing the slope of a logarithmic plot of the release-to-birth ratios (r/b) versus isotope decay constants, the dominant mechanism of fission gas release can in principal be determined. In practice, metallic fuel element breaches in the plenum and in the fuel column both show the stored gas type of release behavior in the early stages (r/b slope= -1). Later (~3 to ~5 days) the gas from the fuel column breach is released by diffusion via interconnected porosity which gives a slope of -0.5. Future efforts in this area is to develop an on-line diagnostic tool as a quick and accurate means of determining the type and number of breaches that are active in an LMR core at any given time.

4. Conclusions

1) The evolution of metallic fuel design has led IFR fuel designers to use fuel smeared densities, plenum-to-fuel volume ratios, and cladding materials that allow burnups near 20 at. %.

2) Based on the results of lead tests of IFR U-Pu-Zr fuel clad with the D9 and HT9 alloys, several irradiation tests were conducted to investigate the effects of various design, operating and fabrication variables on fuel performance.

3) Irradiation tests of U-Zr blanket fuel have demonstrated good performance characteristics at an interim burnup level.

4) Casting fuel into consumable zirconium tubes can reduce quartz mold waste and possibly reduce axial growth in those elements.

5) Breaches in metallic fuel elements have been proven benign. An analytical effort has been initiated that could lead to an on-line method for detecting numbers and types of metallic fuel breaches in an LMR.

References

[1] L. C. Walters, B. R. Seidel and J. H. Kittel, Nucl. Tech. 65 (1984) 179.

[2] R. G. Pahl, R. S. Wisner, M. C. Billone and G. L. Hofman, in: Proc. of the 1990 International Fast Reactor Safety Meeting (ANS, Snowbird, 1990); Vol IV, p. 129.

[3] Y. I. Chang, Nucl. Tech. 88 (1989) 129.

[4] J. M. Kramer and T. H. Bauer, in: Proc. of the 1990 International Fast Reactor Safety Meeting (ANS, Snowbird, 1990), Vol IV, p. 145.

[5] H. Tsai, in: Proc. of the 1990 International Fast Reactor Safety Meeting (ANS, Snowbird, 1990), Vol II, p. 257.

[6] R. G. Pahl, C. E. Lahm, H. Tsai, and M. C. Billone, in: Proc. of the International Conference on Fast Reactors and Related Fuel Cycles (Kyoto,1991), Vol III, P.1.17-1.

[7] B. R. Seidel, D. B. Tracy, and V. Griffiths, "Apparatus for Injection Casting Metallic Nuclear Energy Fuel Rods," U. S. Patent No. 5,044,811, September 3, 1991.

[8] R. G. Pahl, G. L. Batte', R. Mikaili, J. D. B. Lambert and G. L. Hofman, in: Proc. of the International Conference on Fast Reactors and Related Fuel Cycles (Kyoto,1991), Vol. III, P.1.19-1.

[9] G. L. Batte' and G. L. Hofman in: Proc. of the 1990 International Fast Reactor Safety Meeting (ANS, Snowbird, 1990),Vol IV, p. 207.

Table 1. Design data for the HT9-clad elements in the X441, X447 tests

	X441	X447
Peak linear power, Kw/m	51	33
Peak inside cladding temperature	660°C	660°C
Element length, cm.	74.9	74.9
Plenum vol./ fuel vol.	~1.1 to ~2.1	~1.5
Clad wall thickness, mm	0.38	0.38
Clad outer diameter, mm	5.84	5.84
Fuel alloy, wt.%	U-19Pu-6,10,14 Zr	U-10Zr
Fuel Smeared Density, %	70,75,85	75

Table 2. Summary of X441 cladding strain data

% Smeared density	Fuel alloy	Plenum/fuel volume ratio	% Diametral clad strain
75	U-19Pu-10Zr	1.1	0.32
75	U-19Pu-10Zr	1.5	0.28
75	U-19Pu-10Zr	2.1	0.17
75	U-19Pu-6Zr	1.5	0.27
75	U-19Pu-14Zr	1.5	0.25
70	U-19Pu-10Zr	1.5	0.22
85	U-19Pu-10Zr	1.3	1.66, 2.28

Table 3. Summary of blanket element design parameters and post-irradiation examination results

Test ID	Fuel alloy	Smear density	Clad wall mm.	Plenum to fuel ratio	Peak burnup at. %	% Axial growth	% Clad diam. strain
X431	U-2Zr	85%	0.38	1.93	1.07	5.09	0.25*
X431	U-2Zr	90%	0.51	1.82	1.06	2.77	0.36
X431	U-6Zr	85%	0.38	1.93	1.22	4.04	0.26
X431	U-6Zr	90%	0.51	1.82	1.22	2.29	0.32
X431	U-10Zr	85%	0.38	1.93	1.38	4.95	0.20
X431	U-10Zr	90%	0.51	1.82	1.36	2.73	0.30
X432	U-2Zr	85%	0.38	1.93	1.35	5.77	0.30*
X432	U-2Zr	90%	0.51	1.82	1.38	3.26	0.32
X432	U-6Zr	85%	0.38	1.93	1.56	3.91	0.21
X432	U-6Zr	90%	0.51	1.82	1.57	2.38	0.32
X432	U-10Zr	85%	0.38	1.93	1.78	4.82	0.22
X432	U-10Zr	90%	0.51	1.82	1.70	2.75	0.26

* This strain was measured outside of the region of non-uniform deformation discussed in Section 3.c
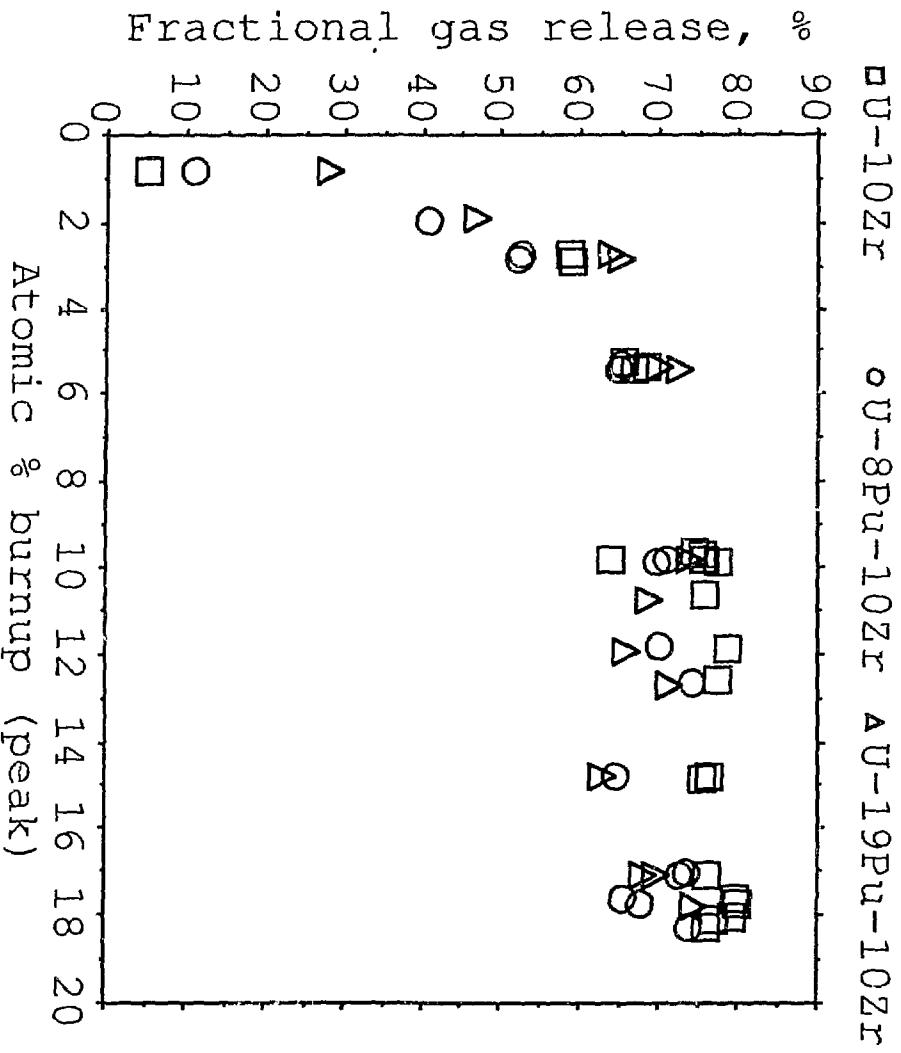
Figure Captions

Figure 1. Fractional gas release curve for typical IFR
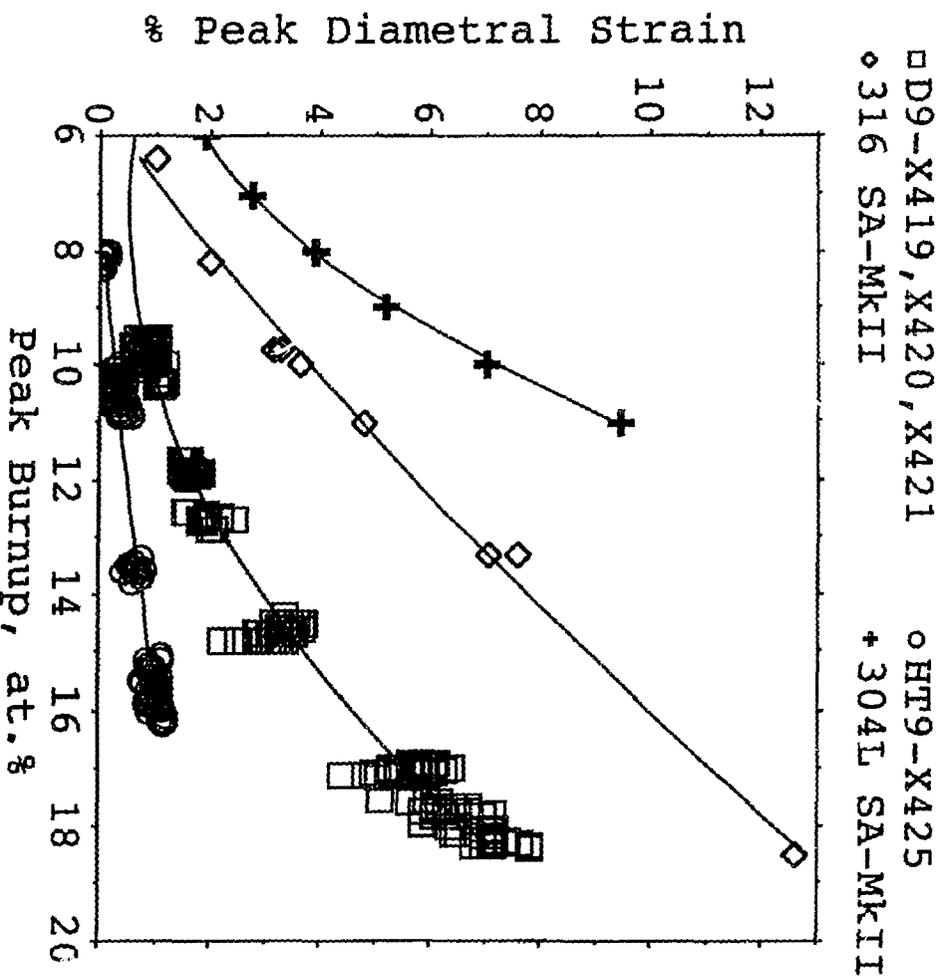   metallic fuel [2].

Figure 2. Cladding strain behavior for early EBR-II driver
           fuel (Mk-II type) and experimental IFR metallic
           fuel.

Figure 1. Fractional gas release curve for typical IFR metallic fuel [2].

Figure 2. Cladding strain behavior for early EBR-II driver fuel (Mk-II type) and experimental IFR metallic fuel.